© 2014. Published by The Company of Biologists Ltd | The Journal of Experimental Biology (2014) 217, 3615-3628 doi:10.1242/jeb.105502

RESEARCH ARTICLE

Enhanced sensory sampling precedes self-initiated locomotion in an electric fish

James J. Jun[1,2,3,*,‡], André Longtin[1,2,3] and Leonard Maler[2,3]

ABSTRACT

Cortical activity precedes self-initiated movements by several seconds in mammals; this observation has led into inquiries on the nature of volition. Preparatory neural activity is known to be associated with decision making and movement planning. Self-initiated locomotion has been linked to increased active sensory sampling; however, the precise temporal relationship between sensory acquisition and voluntary movement initiation has not been established. Based on long-term monitoring of sensory sampling activity that is readily observable in freely behaving pulse-type electric fish, we show that heightened sensory acquisition precedes spontaneous initiation of swimming. *Gymnotus* sp. revealed a bimodal distribution of electric organ discharge rate (EODR) demonstrating down- and up-states of sensory sampling and neural activity; movements only occurred during up-states and up-states were initiated before movement onset. EODR during voluntary swimming initiation exhibited greater trial-to-trial variability than the sound-evoked increases in EODR. The sampling variability declined after voluntary movement onset as previously observed for the neural variability associated with decision making in primates. Spontaneous movements occurred randomly without a characteristic timescale, and no significant temporal correlation was found between successive movement intervals. Using statistical analyses of spontaneous exploratory behaviours and associated preparatory sensory sampling increase, we conclude that electric fish exhibit key attributes of volitional movements, and that voluntary behaviours in vertebrates may generally be preceded by increased sensory sampling. Our results suggest that comparative studies of the neural basis of volition may therefore be possible in pulse-type electric fish, given the substantial homologies between the telencephali of teleost fish and mammals.

KEY WORDS: Weakly electric fish, Voluntary movement, Active sensing, Decision making, Readiness potential, Volition

INTRODUCTION

Volition is generally considered as a defining human faculty; but the outcome of a voluntary decision can be predicted by brain activity even before a subject's conscious awareness (Libet et al., 1983; Soon et al., 2008; Desmurget and Sirigu, 2012), and a gradual increase in neural activity preceding voluntary movement is observed in several species (Kornhuber and Deecke, 1965; Fried et al., 2011; Romo and Schultz, 1987). Preparatory neural activities for voluntary movements involve movement planning and decision making (Kaufman et al., 2010), and voluntary control of active sensory sampling accompanies heightened spatial attention (Winkowski and Knudsen, 2006; Ulanovsky and Moss, 2008). Here, we show that enhanced sensory sampling precedes the voluntary decision to move in an animal model that exhibits a readily observable and quantifiable sensory acquisition rate. In addition to demonstrating preparatory increases in sensory sampling, our results imply close linkages between sensory sampling and neural activity in a weakly electric fish, suggesting that they are also associated with voluntary decision making.

Humans can make conscious decisions to initiate movement (Haggard, 2008) without external sensory stimuli (Sokolov, 1990). Cortical recordings reveal that neural activity precedes the time when a conscious decision to act is reported (Kornhuber and Deecke, 1965; Libet et al., 1983; Soon et al., 2008), raising questions as to how neural activity relates to conscious decision making and the initiation of voluntary actions. Whereas prior work has shown neural activity preceding voluntary actions in primates capable of advanced cognition (Romo and Schultz, 1987; Kato et al., 1995; Kaufman et al., 2010), here we demonstrate the same pattern in an aquatic vertebrate whose last common ancestor to primates lived more than 450 million years ago. We propose that volition may therefore be a primitive capability of vertebrate brains that precedes the advanced cognitive capacities of primates.

Animals actively sample their environment using, for example, whisking, sniffing and saccadic eye movements; these active sensing behaviours (Nelson and MacIver, 2006; Kleinfeld et al., 2006; Otero-Millan et al., 2008; Wachowiak, 2011) occur more frequently during periods of active exploration (Poulet and Petersen, 2008; Schroeder et al., 2010). Gathering of sensory information can guide movement decisions to be made later, but the precise temporal relationship between volitional acts and sensory sampling is still not known; for example, does active sensing increase before, together with or after self-initiated movements? A general answer is here suggested based on pulse-type weakly electric fish, such as *Gymnotus* sp. These fish emit brief (~1 ms) electric organ discharge (EOD) pulses that stimulate cutaneous electroreceptors; each pulse corresponds to a discrete active sampling event. Objects in the fish's environment distort their EOD-generated electric field, resulting in localized electric images that, in the dark, are the primary sensory basis for navigation and prey capture. Unexpected stimuli will cause an increase in the EOD rate (EODR; novelty response) and therefore the putative sampling rate of the tuberous electrosensory system (Caputi et al., 2003; Pluta and Kawasaki, 2008). Previous work has shown that pulse-type weakly electric fish compare the reafferent electrosensory image induced by each EOD pulse with a stored template derived from previous electrosensory input (Heiligenberg, 1980; Hopkins, 1983; Moller, 1995; Post and von der Emde, 1999; Caputi et al., 2003). Caputi and colleagues demonstrated that a

[1]Department of Physics, University of Ottawa, Ottawa, ON, Canada, K1N 6N5. [2]Department of Cellular and Molecular Medicine, University of Ottawa, Ottawa, ON, Canada, K1H 8M5. [3]Centre for Neural Dynamics, University of Ottawa, Ottawa, ON, Canada, K1N 6N5.
*Present address: Janelia Research Campus, Howard Hughes Medical Institute, Ashburn, VA 20147, USA.

‡Author for correspondence (jamesjun@gmail.com)

Received 17 March 2014; Accepted 31 July 2014

List of abbreviations

CDF	cumulative distribution function
CV	coefficient of variation
EOD	electric organ discharge
EODA	EOD acceleration
EODR	EOD rate
IPI	inter-pulse interval
KS	Kolmogorov–Smirnov
PC1	first principal component
PSD	power spectral density
SPL	sound pressure level

template of the electrosensory input develops over many EOD pulses and that a changed input for only one EOD pulse is sufficient to trigger a novelty response. Further, the magnitude of the novelty response undergoes experience-dependent habituation that is inversely proportional to the inter-stimulus interval (Barrio et al., 1991; Post and von der Emde, 1999; Caputi et al., 2003). We conclude that each EOD constitutes a discrete sampling event and that EODR is therefore a direct measure of sampling rate over some time interval. Pulse-type electro-sensation thus offers a distinct experimental advantage because each sampling event can be readily and non-invasively monitored from an unrestrained animal (Jun et al., 2012; Jun et al., 2014). In gymnotiform species, EOD pulses are directly driven by a hindbrain pacemaker that is modulated by diencephalic and medullary prepacemaker activity (Heiligenberg et al., 1981; Kawasaki et al., 1988; Dye, 1988; Metzner, 1993; Caputi et al., 1993; Zupanc and Maler, 1997; Wong, 1997; Comas and Borde, 2010). Previous studies of the electromotor circuitry (Caputi et al., 1993; Wong, 1997; Giassi et al., 2012), functional stimulation of an electromotor thalamic nucleus (Comas and Borde, 2010) and drug injection in the pallium (Santana et al., 2001) all indicate a strong modulation of the EODR from the forebrain. Thus, the net activity of the higher level neural populations projecting to the EOD pacemaker can be inferred from the time derivative of EODR, or EOD acceleration (EODA) (Metzner, 1993; Metzner, 1999; Arnegard and Carlson, 2005; Pluta and Kawasaki, 2008).

RESULTS

Behavioural two states

In this part of the investigation, we demonstrate that *Gymnotus* sp. spontaneously switches between two distinct behavioural states: a resting (immobile) down-state with a low EODR and an active (mobile) up-state with a higher EODR. We show that the transition to a higher EODR precedes the onset of self-initiated movement.

We studied the fish's spontaneous behaviours in a featureless, dark and quiet environment (Fig. 1A) (Jun et al., 2014) devoid of objects. *Gymnotus* sp. is nocturnal and, in a lit environment, is mostly immobile (Fig. 1B) with a low basal level of EOD discharge (Fig. 1C). However, in the dark, the basal EODR of stationary fish significantly increased [48 h of total observation; $P<10^{-12}$, paired Kolmogorov–Smirnov (KS) test]. Our analysis was therefore confined entirely to observations taken in a completely dark environment. Despite the absence of external stimuli, fish spontaneously switched between periods of inactivity and of active swimming (Fig. 1D) and the EODR of each animal also rapidly switched between lower and higher rates (Fig. 1E). During the periods of higher EODR, the animal is sampling its environment more frequently than when in the lower EODR state. We therefore considered high and low EODR periods as distinct sensory states with the high EODR state corresponding to a period of higher sensory sampling. Long-term observation (4.5–12 h day^{-1}, total observation time of 207 h from five animals) of spontaneous behaviours revealed that the switching of EODR is tightly coupled to movement (Fig. 1F; supplementary material Movie 1), and that the EODR does not simply reflect the circadian cycle (Lissmann, 1965). Two distinct clusters in the joint histogram of the EODR and activity level (Fig. 1G), confirm a tight correlation between sensory and behavioural states (Table 1). For all animals, movements only occurred in association with higher EODR. Remarkably, the EODR increased up to 5 s before a spontaneous movement (Fig. 1E; supplementary material Movie 2). In almost all cases (92.1%) and in all animals tested, the increasing EODR transition preceded the spontaneous movement onset (Table 2); the remaining cases (7.9%) are most likely due to the finite temporal precision (σ=0.1 s) of the movement onset detection (see Materials and methods). Because increases in EODR must be due to increased neural activity of neurons providing descending input to the pacemaker nucleus, the increase in EODR implies a change in neural activity. Thus, as is the case for self-initiated movements in humans (Kornhuber and Deecke, 1965; Libet et al., 1983; Soon et al., 2008), altered neural activity precedes motor activity by up to several seconds. Importantly, we also conclude that heightened active sensory sampling precedes movement.

Because of the binary nature of sampling rate and activity level and their rigid correlation, we refer to an active period with high sampling rate as an up-state and an inactive period with low sampling rate as a down-state. We separated the down- and up-states (Fig. 2A) according to the first principal component (PC1) of the EODR and activity level (Fig. 1G,H). As illustrated in Fig. 1G, the principal components analysis rotates the axes of the activity level versus EODR variables graph so as to find variables (components) that are statistically independent; further, the method gives a 'first' principal component that accounts for most of the variability in both data sets. The PC1 explained 90±3% of the total variance; this analysis suggests that a single neural control mechanism is mainly (~90%) responsible for both aspects of the down- to up-state transition. We therefore hypothesize that, despite the variable time lag between them, the increase in EODR and onset of movement are triggered by the same neural mechanism. After the separation, transient states were removed by merging (Fig. 2A,B; see Materials and methods). The EODR and activity level were normalized across different days and individuals (Fig. 1I) by mapping their median values during down- and up-states to zeros and ones, respectively (Fig. 2C).

The sensory sampling activities showed marked differences between the down- and up-states (i.e. without and with movement). In all animals tested, the EODR and EODA distributions significantly differed between the two states ($P<10^{-12}$, paired KS test, α=0.05, 27–72 h; see Table 1). The EODR distributions were clearly separated with minimal overlap (Fig. 3A), and the EODR was significantly higher during active periods in all animals tested (Fig. 3B, Table 1). In both states, the modes of the EODA distributions were negative (Fig. 3C, right), as expected from the generally fast rise followed by slow decay of the EODR (Fig. 3D). The EODA distribution was wider during up-states (Fig. 3C, left), indicating greater temporal modulation of the sensory sampling rate during active movements. In fact, the EOD pulse train exhibited greater temporal variability during up-states according to the Fano factor analysis (Fig. 3E); the Fano factor quantifies the mean-normalized count variability of the EOD pulses as a function of the time window and thus clearly demonstrates that the EODR is far more variable during up-states. These findings suggest that there exist two disjointed states of active sensory sampling, that transitions to the higher sampling rates (i.e. to an up-state) are tightly coupled

The Journal of Experimental Biology (2014) doi:10.1242/jeb.105502

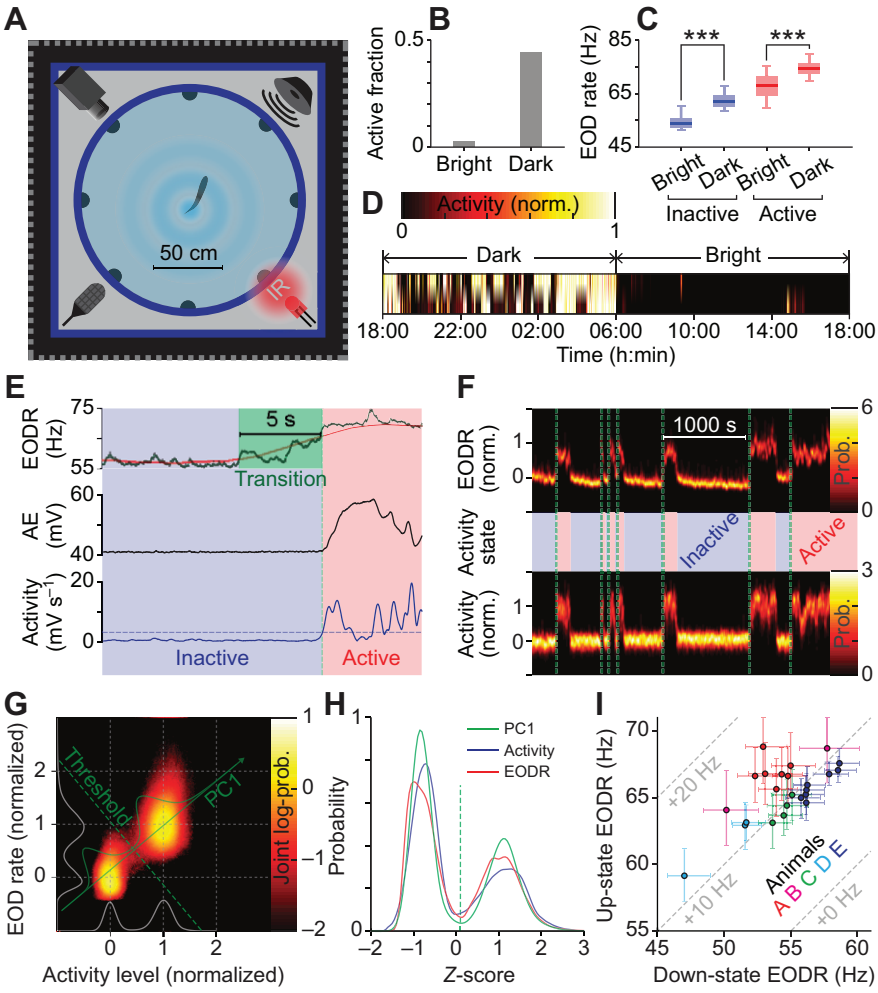

Fig. 1. Two behavioural and attentional states in *Gymnotus* sp. (A) Experimental tank in a sensory-isolation chamber with infrared (IR) lighting. Electric organ discharge (EOD) signal was captured by eight dipoles symmetrically placed around the edge of the tank to monitor the EOD rate (EODR) and movement activity; a video camera also directly captured movement. Subwoofers delivered random stimuli during a sensory-evoked condition and a microphone was used to record possible noise contamination. (B) Fraction of active periods under bright and dark conditions. (C) Box plots of EODR distributions (displaying 5th, 25th, 50th, 75th and 95th percentiles) during inactive (blue) and active periods (red) under bright and dark conditions. (D) Activity levels recorded for 48 h indicate predominance of activities in darkness. All data in B–D were obtained from animal A continuously for 48 h (two rows indicate two consecutive days). Vertical colour bars indicate periods of active movements interrupted by resting periods (black). (E) Example traces of the EOD rate (EODR), EOD amplitude envelope (AE), and activity level during a spontaneous movement initiation. Moving average of the EODR (red trace) started to increase 5 s before movement onset (dashed green line). (F) Probability density (heat map) of the normalized EODR and activity level over time, which randomly switched between two states. Movement onset (dashed green lines) closely coincided with the EODR transition onset. (G) Joint log-probability density (heat map) of the normalized EODR and activity level and their first principal component (PC1; green trace) were used to clearly separate the down- and up-states by applying a threshold (dashed line). (H) *Z*-score distributions of the activity level, EODR and their first principal component (PC1). Dashed green line (local minima of the PC1 distribution) indicates the state-segregation threshold for PC1. (I) Scatter plot of the up- versus down-state EODR from multiple days and animals. Black circles indicate the median, and error bars indicate the 25th and 75th percentiles. Each colour represents a different individual.

to and precede movements, and that the sensory sampling rate is highly modulated when associated with movement.

Preparatory increase in the sensory sampling rate

Here, we compared the increase in EODR that precedes a self-initiated movement versus the increase associated with a stimulus (acoustic)-evoked movement. We show that stimulus-evoked EODR increases are stereotyped and may be reflex responses to a strong, unexpected sound. In contrast, the EODR increases preceding self-initiated movements have highly variable timing and are clearly not reflexes associated with movement.

Sustained preparatory neural activities preceding voluntary movements have been reported in humans (Kornhuber and Deecke, 1965; Libet et al., 1983; Soon et al., 2008) and monkeys (Romo and Schultz, 1987; Kato et al., 1995; Kaufman et al., 2010). Here, however, we further demonstrate that the increased neural activity preceding self-initiated movement is also associated with a heightened sensory sampling (EODR) that precedes movement onset. In addition, the temporal relationship between sensory sampling and motor activities exhibited striking differences for spontaneous versus sound-evoked movements. In the sound-evoked condition, loud acoustic stimuli [143 dB sound pressure level (SPL) root-mean-squared (rms), 150 Hz pure tone, 0.5 s or 1 s duration] were delivered at random intervals (4–6 min inter-stimulus intervals) to trigger startle responses (Korn and Faber, 2005). We only analysed evoked trials when the acoustic stimuli triggered significant movements of a resting animal (70% of all trials). The initial rise of EODR preceded a movement onset significantly earlier

The Journal of Experimental Biology (2014) doi:10.1242/jeb.105502

Table 1. Data summary for the behavioural two states

	A	B	C	D	E
Total recording time (h)	62.1	10.7	34.9	27.4	71.7
Probability of up-state	26.4%	57.9%	65.8%	71.4%	88.9%
Correlation between EODR and activity level	0.832, $P<10^{-12}$	0.815, $P<10^{-12}$	0.816, $P<10^{-12}$	0.817, $P<10^{-12}$	0.726, $P<10^{-12}$
Up-state EODR (Hz)	67.1±3.8	66.2±5.6	64.2±3.4	62.5±3.5	66.3±2.5
Down-state EODR (Hz)	53.6±2.5	48.9±6.1	54.3±2.4	48.7±3.1	56.9±3.3
KS test[a] for EODR distributions between down- and up-states	$P<10^{-12}$	$P<10^{-12}$	$P<10^{-12}$	$P<10^{-12}$	$P<10^{-12}$
Up-state EODA (Hz s^{-1})	–0.1±6.5	–0.5±11.7	–0.2±7.5	–0.2±7.9	–0.1±6.0
Down-state EODA (Hz s^{-1})	–0.0±4.3	–0.1±6.9	0.0±4.9	0.1±5.0	0.1±6.0
KS test[a] for EODA distributions between down- and up-states	$P<10^{-12}$	$P<10^{-12}$	$P<10^{-12}$	$P<10^{-12}$	$P<10^{-12}$

Data are given for animals A–E. Data for up- and down-state EODR and EODA are means ± s.d.
EODR,electric organ discharge rate; EODA, electric organ discharge acceleration.
[a]KS test refers to the paired Kolmogorov–Smirnov test (*kstest2* function in MATLAB).

in the spontaneous condition compared with the evoked condition (Fig. 4A, Table 2). Likewise, the trial-averaged EODA (slope of the EODR) during spontaneous transitions became positive ~1.5 s earlier than during evoked transitions (Fig. 4B). Under both conditions, the peak of the trial-averaged EODA coincided with a movement onset (Fig. 4B, bottom). To precisely align the trials for averaging, we visually confirmed the movement-onset times determined from the activity level in a subset of trials (Fig. 5A–F; see Materials and methods). The movement-triggered averages of the activity level showed no significant baseline activity before movement onset under both conditions (Fig. 4C), thus confirming that the differences in the EODR and EODA between the spontaneous and evoked conditions cannot be attributed to the differences in the baseline activity levels. The differences in the EODR or EODA between the two conditions could not be explained by the differences in movements, because the activity levels under the two conditions did not significantly differ from each other (Fig. 4C). We also observed no significant increase of the background acoustic noise before self-initiated movements (Fig. 4D), validating that these transitions were indeed spontaneous.

To quantify the temporal relationship between the sensory and motor transitions, the time intervals between the initial EODR rise and movement onset (transition latency) were compared between the spontaneous and evoked transitions. The transition latency distributions for spontaneous transitions had longer median latencies and wider spreads than for evoked transitions in all animals tested (Fig. 4E). The EODR switched to up-states significantly before self-initiated movements (Table 2), with highly variable transition latencies, whereas acoustic stimuli caused an immediate increase of the EODR, and movements quickly followed in a stereotyped (i.e. less variable) manner. Fig. 4F shows that animals were more likely to initiate movements as they spent longer time in the EODR up-state (EODR >0.4). The probabilistic temporal relationship between the spontaneous switching of the sensory sampling rate and the movement-initiation rules out an automatic coupling between the two. Fig. 4G compares two types of trials where spontaneous EODR up-transitions led to either movement initiation (moved, N=456) or down-transitions without movement (aborted, N=1,198) from the same animal. The mean trajectory of the aborted transitions reached not much beyond (<0.5) the EODR threshold (0.4) before falling back, whereas the transitions that led to movement nearly reached the median up-state EODR (1.0) before crossing the activity threshold (0.2). Fig. 4G thus confirms that the EODR up-transition generally precedes spontaneous movement initiation when they are

Table 2. Data summary for the transition latency and across-trial variability

	A	B	C	D	E
No. spontaneous transitions	174	204	323	203	404
No. evoked transitions (all)	102	28	89	58	19
No. evoked transitions (moved)	86	21	33	49	19
Duration of sound stimulus (s)	0.5	1	1	1	1
Spontaneous up-transition latency (s)	0.67±0.75	0.38±0.48	0.52±0.63	0.33±0.55	0.41±0.46
Evoked up transition latency (s)	0.21±0.13	0.03±0.08	0.09±0.07	0.04±0.05	0.07±0.02
KS test[a] between spontaneous and evoked transition latency distributions	$P<10^{-12}$	$P<10^{-12}$	$P<10^{-12}$	$P<10^{-12}$	$P<10^{-12}$
Probability of EODR up-transition preceding spontaneous movement onset	86.4%	95.7%	97.9%	82.3%	93.1%
Across-trial EODR s.d.[b] during spontaneous transitions	0.27±0.03	0.29±0.03	0.29±0.02	0.26±0.03	0.29±0.02
Across-trial EODR s.d. during evoked transitions[a]	0.14±0.02	0.17±0.05	0.19±0.03	0.17±0.04	0.14±0.04
Lilliefors test for EODR during spontaneous transitions[c]	$P>0.05$	$P>0.05$	$P>0.05$	$P>0.05$	$P>0.05$
Lilliefors test for EODR during evoked transitions[c]	$P>0.05$	$P>0.05$	$P>0.05$	$P>0.05$	$P>0.05$
F-test for equal variances of EODR between spontaneous and evoked transitions[c]	$P<10^{-3}$	$P<10^{-2}$	$P<10^{-3}$	$P<10^{-2}$	$P<10^{-2}$

Data are given for animals A–E. Latency data are means ± s.d.
EODR, electric organ discharge rate.
[a]KS test refers to the paired Kolmogorov–Smirnov test (*kstest2* function in MATLAB). [b]Trial-to-trial EODR s.d. was computed when the trial-averaged EODR reached the transition threshold (0.4). 95% bootstrap confidence interval is given. [c]The EODR values were sampled when the trial-averaged EODR reached the transition threshold (0.4).

The Journal of Experimental Biology (2014) doi:10.1242/jeb.105502

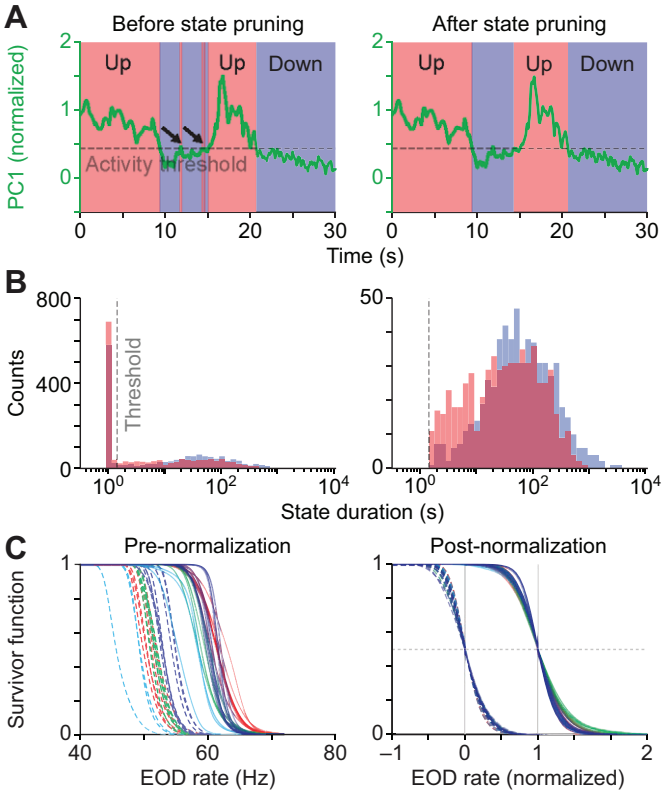

Fig. 2. State pruning by merging and data normalization. (A) The first principal component of the EODR and activity level (PC1) over time (green trace), and resulting states after the state segregation (red, up-state; blue, down-state). Dashed black line represents the PC1 segregation threshold, and black arrows in the left panel indicate transient up-states (left) to be merged into the down-state (right). (B) Histogram of the down- (blue) and up-state (red) durations before (left) and after (right) the state pruning procedure from the same animal (4 days pooled). Dashed grey lines indicate a threshold for the minimum state duration (1.5 s), which was set at the first local minimum of the up-state duration histogram (left). (C) Normalization of data across multiple days and animals. Survivor functions of the EODR are shown during down- (dashed lines) and up-states (solid lines) before (left) and after (right) the normalization procedure. Each animal is represented by a different colour.

sufficiently strong and long-lasting. We conclude that external sensory stimuli trigger an immediate stereotyped reflex movement (Korn and Faber, 2005) and a near-simultaneous associated increase in the sensory sampling rate (Caputi et al., 2003; Comas and Borde, 2010); in contrast, self-initiated movements are preceded by a sustained increase in the sensory sampling with highly variable transition latencies and without any apparent sensory trigger.

Preparatory increase in the sensory sampling variability

In this section, we show that the EODR preceding and accompanying self-initiated movement is very variable across trials. The EODR can be considered as a proxy of the neural activity driving the EOD medullary EOD pacemaker (Comas and Borde, 2010) and we conclude that, as is the case in primates, neural activity associated with voluntary movement is highly variable from trial to trial. We also analysed the variability of stimulus-evoked EODR increases and show that they are much less variable, corresponding to their more reflex nature (see above).

Previous studies reported increasing trial-to-trial variability in neural activities leading up to a voluntary movement onset (Steinmetz and Moore, 2010; Churchland et al., 2011), whereas stimulus onset quenches neural variability (Steinmetz and Moore, 2010; Churchland et al., 2010; Litwin-Kumar and Doiron, 2012). As the EODR reflects the neural activity associated with sensory sampling, we examined how EODR activity varied between trials during spontaneous and evoked transitions as a proxy for the variation in neural activity. Fig. 6A shows time-evolutions of the normalized EODR distributions. The distributions associated with spontaneous movements (Fig. 6A, left) exhibited greater trial-to-trial variability than the sound-evoked responses (Fig. 6A, right). EODR traces of 10 randomly selected trials from the same animal showed greater deviations from the trial-averaged trace during spontaneous transitions (Fig. 6B), and across-trial s.d. of the normalized EODR confirms greater variability during spontaneous transitions (Fig. 6C). All sound-evoked trials having a down-state baseline were pooled regardless of whether or not movements were elicited, as their initial EODR responses were similar within 0.5 s of the stimulus onset. We separately computed the trial-to-trial variability for each animal (Fig. 7A,B) to rule out the variance contributed by individual differences. In all animals tested, increases in the sampling rate variability (s.d. EODR) preceded self-initiated movements, and decreases followed shortly thereafter (Fig. 6C, left; Fig. 7A).

During the course of transitions, across-trial s.d. of the EODR strongly depended on the mean EODR (Fig. 6D, Fig. 7C). To rule out a possible influence of having different mean values on the across-trial variability, we directly compared the s.d. of EODR

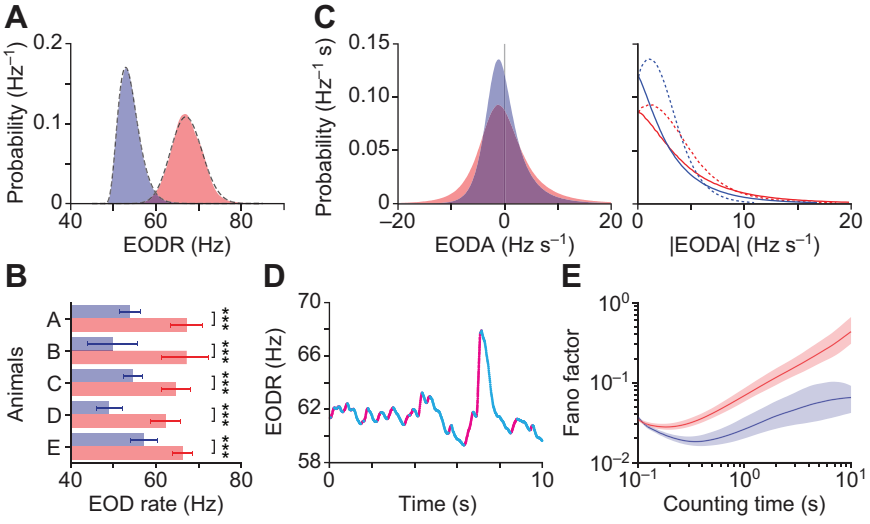

Fig. 3. State-dependent sensory sampling activities. (A) Distributions of the EODR showed distinct sensory sampling rates during down- and up-states from a spontaneously behaving animal. Red/blue indicates down/up-states throughout this figure. Dashed black lines indicate shifted log-normal distribution fitting. (B) Mean EOD rates exhibited significant differences between the two states in all four animals; error bars indicate ±1 s.d.; ***P<0.001. (C) Left, distribution of the EOD acceleration (EODA=dEODR/dt) showed wider spread during up-states, indicating greater temporal modulations of the sensory sampling. Right, positive (solid lines) and negative (dashed lines) sides of the EODA distributions were superimposed to depict the asymmetry in the increasing and decreasing phases of the EODR. (D) An example trace of the EODR showed quicker rising (magenta line) and slower falling (cyan line) phases during an up-state. (E) Fano factors of the EOD pulse counts during a down-state (200 s long) followed by an up-state (200 s long); shaded areas indicate 95% bootstrap confidence intervals. All data in A and C–E were obtained from the same animal.

The Journal of Experimental Biology (2014) doi:10.1242/jeb.105502

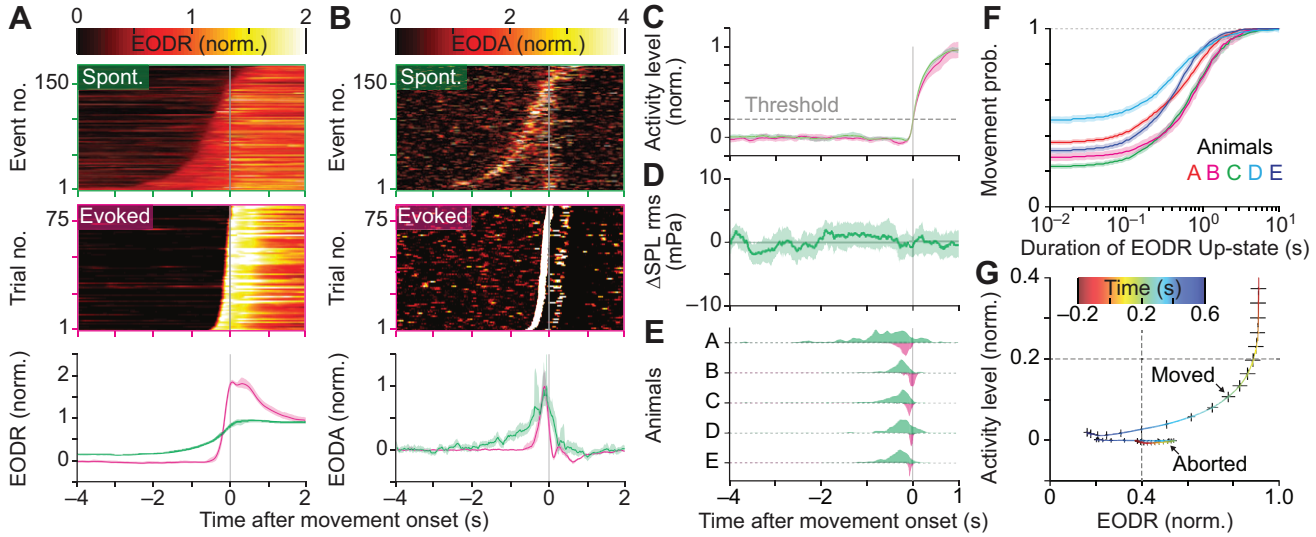

Fig. 4. Increase in the sensory sampling rate precedes voluntary movement. (A,B) Pseudo-colour plots of the normalized EODR (A) and the EODA (B) time courses during spontaneous (top) and sound-evoked (middle) transitions. Time 0 indicates the movement onset, and trials are ordered by their EODR up-transition onsets. Bottom, trial-averaged EODR and EODA normalized by the peak; both exhibited striking differences between spontaneous (green traces) and evoked (magenta traces) transitions. (C) Activity level time courses averaged across all trials showed no significant differences between the spontaneous (green) and evoked (magenta) trials (all animals pooled). Dashed grey line indicates the activity threshold (0.2) for the movement-onset detection. (D) No significant increases in the background noise were observed before spontaneous movement onset. ΔSPL, trial-averaged underwater sound pressure level (SPL) after baseline subtraction. (E) Comparisons of the distributions between spontaneous (green shading) and evoked (magenta shading) transitions demonstrate significantly longer EODR transition latencies for spontaneous compared with sound-evoked transitions in all animals tested (Table 2). (F) The probability of initiating movement increased as the duration threshold of the EODR up-state increased in all animals. (G) Comparison of the two trajectories (moved versus aborted) averaged across trials that crossed the EODR up-state threshold (0.4). Dashed horizontal line indicates the movement threshold, and dashed vertical line indicates the EODR threshold. Colours represent the time since the threshold crossing. The error bars or colour shading indicate 95% bootstrap confidence intervals. All data in A, B and G were obtained from the same animal; all tested animals were pooled for C and D. Solid lines and shaded areas indicate the trial-averaged mean ± s.e.m.

between the spontaneous and evoked transitions when their mean values were both equal to the transition threshold (0.4). For a given trial-averaged EODR, the across-trial s.d. during spontaneous transitions generally exceeded that of the evoked transitions in all animals tested (Fig. 6E, Fig. 7C). When the trial-averaged normalized EODR (mean EODR) crossed the transition threshold, the normalized EODR followed a Gaussian distribution in all animals (Lilliefors test, Table 2), and the across-trial s.d. (s.d. EODR) were significantly greater during spontaneous transitions ($P<10^{-2}$, F-test for equal variance; see Table 2).

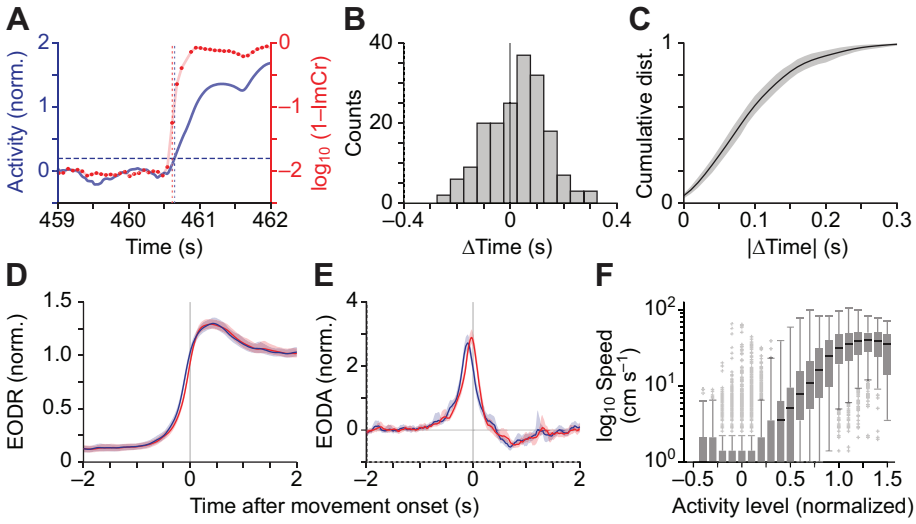

Fig. 5. Visual confirmation of the EOD-based movement onset detection. (A) Example traces of the EOD-based activity level (blue line) and the image correlation (ImCr) measure (red line) during movement onset. Each image frame is represented by a red dot, and joined together for visual aid. Vertical dashed lines indicate movement onset times determined by the two detection methods, and the horizontal dashed line indicates the EOD-based activity threshold (0.2). (B) Distribution of the time differences (ΔT_{move}) between the two movement onset detection methods. (C) Cumulative distribution of the absolute time differences ($|\Delta T_{move}|$). Shaded area indicates 95% bootstrap confidence interval. (D,E) Trial-averaged EODR (D) and EODA (E) time courses computed by the EOD-based (blue) and visual (red) movement onset detection methods agree within ~0.1 s. Shaded areas indicate ±1 s.e.m. (F) Box-plot of the log-speed of the image centroid as a function of the activity level (displaying 5th, 25th, 50th, 75th and 95th percentiles). Medians are indicated by black bars, and outliers are shown as grey crosses. All data in A–F were obtained from animal B.

The Journal of Experimental Biology (2014) doi:10.1242/jeb.105502

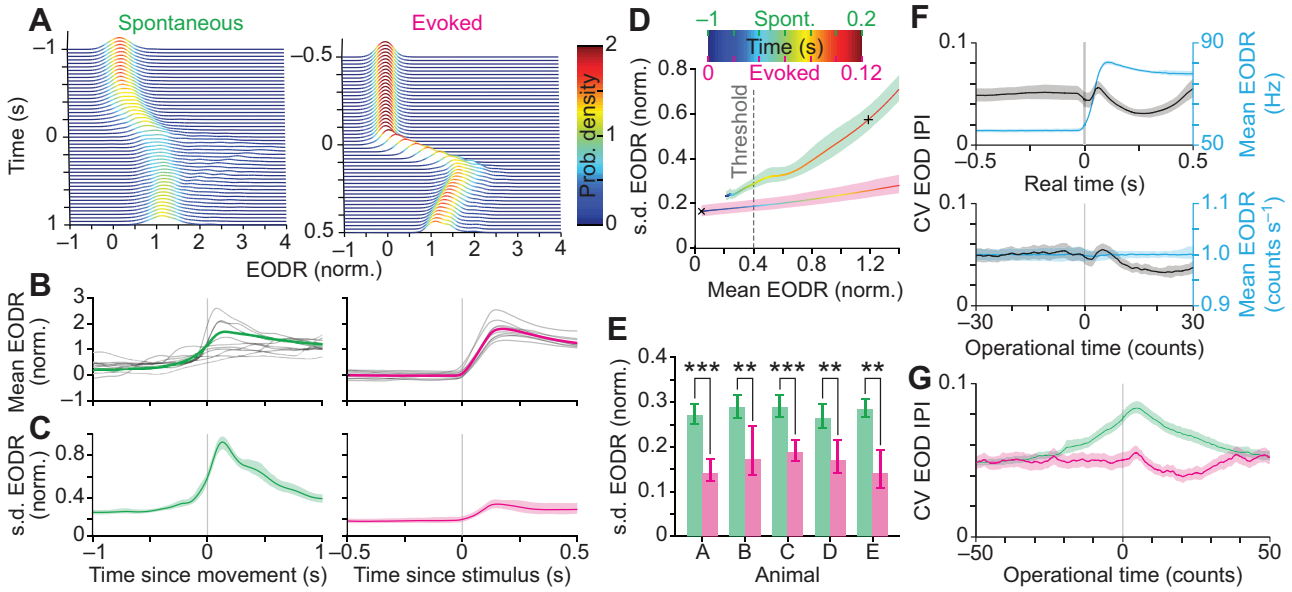

Fig. 6. Increase in the sensory sampling variability precedes voluntary movement. (A) Time-dependent distribution of the EODR during spontaneous transitions (left) exhibited a wider spread than during evoked transitions (right). Colours represent the probability density of the EODR; time 0 indicates the movement or sound onset. (B) EODR time courses from 10 randomly selected trials (grey lines) showed greater deviations from the mean (coloured lines) during spontaneous transitions (left). Green/magenta indicates the spontaneous/evoked conditions throughout this figure. (C) Across-trial s.d. of the EODR reveal greater trial-to-trial variability during spontaneous transitions (left). (D) Comparison of the across-trial s.d. of any given mean EODR confirms greater trial-to-trial variability during spontaneous transitions. Colours represent the time of transition; +, movement onset; x, stimulus onset. All data in A–D were obtained from animal C. (E) In all animals tested, the across-trial s.d. at the transition threshold (dashed grey line in D) exhibited significant differences between the spontaneous and evoked transitions; $^{**}P<0.01$, $^{***}P<0.001$. (F) The coefficient of variation (CV) of the EOD intervals (black lines) declined after stimulus onset, but the mean rate (cyan lines) simultaneously increased (top). The CV was recomputed after applying the time-rescaling procedure (N=98, animal A), which produced a constant mean rate (bottom). IPI, inter-pulse interval. (G) Trial-to-trial variability peaked near the spontaneous movement onset (N=1157, five animals), but declined after stimulus onset (N=291, five animals). All shaded areas indicate 95% bootstrap confidence intervals. The CVs were computed after averaging four successive EOD intervals at 0.1 ms resolution.

The time course of the trial-averaged EODR exhibited large differences between animals and between the spontaneous and evoked conditions (Fig. 7A,B). In order to facilitate pooling of data from different animals, the effect of time-varying mean rate on the across-trial variance was removed by applying a time-rescaling procedure (Brown et al., 2002; Nawrot et al., 2008). This mathematically well-grounded procedure normalizes the time axis of the EODR so that direct statistical comparisons can be made across animals even if their original EODR temporal modulations were different. After applying the procedure, the mean rate became constant in the operational time scale, but the coefficient of variation (CV) of the EOD inter-pulse intervals still exhibited a decline after the stimulus onset (Fig. 6F, bottom). Consistent with the previous findings (Steinmetz and Moore, 2010; Churchland et al., 2010; Churchland et al., 2011; Litwin-Kumar and Doiron, 2012), the trial-to-trial variability of the sensory sampling intervals as measured by the CV (pooled from five animals) peaked near the voluntary movement onset, but declined after the stimulus onset (Fig. 6G). These findings suggest that the time course of sensory sampling variability mirrors the previously reported increase in neural variability preceding a decision to act (Steinmetz and Moore, 2010; Churchland et al., 2011), and the trial-to-trial sampling variability associated with voluntary movements significantly exceeds that of the stimuli-triggered responses.

Spontaneous behavioural transitions

In this part of the investigation, we show that transitions from down- to up-states (and vice versa) occur in a random manner. This is consistent with the idea that voluntary behaviours are unpredictable (Haggard, 2008). We used several statistical methods to prove randomness of down- and up-state durations and transitions. We also demonstrate that down/up transitions were based on an underlying renewal process, i.e. a process with no ‘memory’ so that the duration of a previous down- or up-state did not influence the duration of the next state.

It has been previously proposed that voluntary behaviours are initiated in a random or unpredictable manner (Haggard, 2008). This computational principle indeed held true in the case of spontaneous behavioural state transitions in *Gymnotus* sp., based on the following fractal time-series analyses to uncover their underlying temporal structures from long-term observations. The survivor functions (=1–cumulative density function) of the intervals between two successive down- to up-state transitions (up-transitions) showed approximately linear trends on a lin-log scale (Fig. 8A), and the durations of the down- and up-states followed similar trends (Fig. 8B). The distributions of up-transition log-intervals were well fitted assuming an underlying log-normal density for these intervals (Fig. 8C, Fig. 9A,B, Table 3). The power spectrum of spontaneous up-transition events showed power at all frequencies (Fig. 8D), suggesting no clear periodicity features or characteristic time scale (Proekt et al., 2012).

In addition, we found a lack of predictability based on the history of spontaneous transitions. The joint log-interval histogram of spontaneous up-transitions exhibited no clear structure, indicating a lack of temporal correlation (Fig. 8E). Indeed, little or no correlation was found between pairs of up-transition intervals, state durations and transition latency (Fig. 8F). The Fano factor for spontaneous up-transition counts increased linearly on a log–log scale (Fig. 8G,

The Journal of Experimental Biology (2014) doi:10.1242/jeb.105502

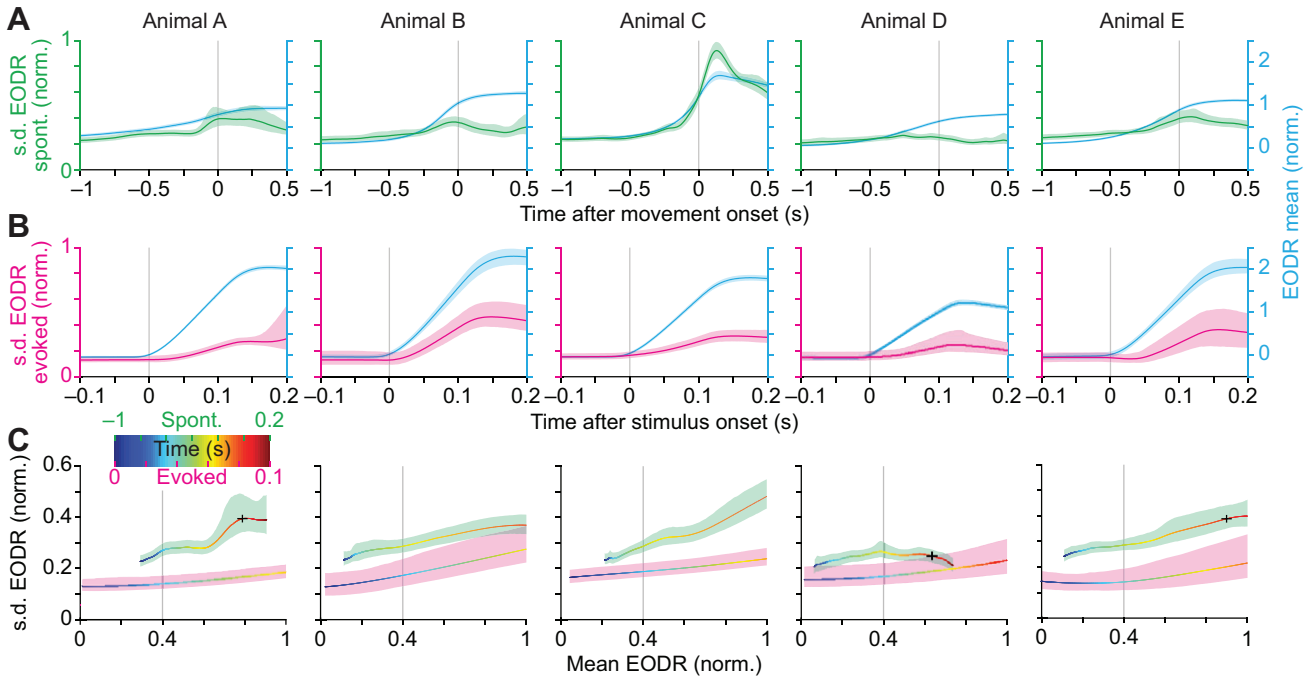

Fig. 7. Trial-to-trial variability and mean of the EODR for each animal during up-transitions. (A) Across-trial mean (cyan traces) and s.d. (green traces) of the EODR for spontaneous transitions as a function of time before and after movement onset. (B) Same as A for evoked transitions as a function of time before and after stimulus onset. The across-trial s.d. are shown as magenta traces. (C) Across-trial s.d. of the EODR as a function of the trial-averaged EODR during spontaneous (green) and evoked transitions (magenta). Shaded areas represent 95% bootstrap confidence interval. Pseudo-colour indicates time during transition; black cross marks the movement onset. The EODR transition threshold (0.4) is indicated by vertical dashed grey lines.

Table 3). To confirm lack of temporal correlation in the spontaneous transitions, we computed the Fano factors for 10 randomly shuffled up-transition intervals, and superimposed them with the original plot (Fig. 8H, Fig. 9C). Within the limit of our observation time window ($10^{0.2}$–$10^{3.5}$ s), the original Fano factors did not significantly differ from those for the shuffled controls in all animals except one (animal D, $t>10^2$ s). After removing slow trends in the data by applying Allan factor analysis (Gebber et al., 2006), no significant differences were found between the original and shuffled data in all animals (Fig. 9D). The Hurst exponents of the spontaneous up-transition counts ranged between 0.52 and 0.63 (Table 3), which is indistinguishable from those produced by a random process with no memory (Hardstone et al., 2012). These metrics all demonstrate that the spontaneous behavioural transitions are not deterministic but, rather, are due to a renewal process with log-normal characteristics.

DISCUSSION

Our results reveal that weakly electric fish exhibit preparatory neural activity up to 5 s before spontaneously initiating movement (Fig. 1E), and that such movements are associated with enhanced sensory sampling evident by the increased EODR. Through behavioural down-to-up transitions, such movements are also correlated with the increased variability of neural activity characteristic of voluntary acts in primates. Preparatory neural activity preceding voluntary movements has been shown to be involved in movement planning (Kaufman et al., 2010) and decision making in primates (Steinmetz and Moore, 2010; Churchland et al., 2011). In *Gymnotus* sp., the higher sensory sampling rates during movement may be attributed to the increased demands on the brain to process the high flow of sensory information induced by self-motion (Nelson and MacIver, 2006). Yet, this cannot explain our observation of increased sensory sampling rates and sampling rate variability that precedes movement onset; if an increase in EODR was only required for gathering more information during movement, it would only have to occur during movement and not before movement was initiated. We propose that the increased sensory sampling and associated neural activity preceding movements are not only for gathering of more information but also involved in the fish making the decision to move and in planning the trajectory of its movement. We therefore hypothesize a direct analogy of preparatory neural activity in primates and that of *Gymnotus sp*. (as seen in the proxy, EODR).

We established a precise temporal relationship between the sensory and motor activities by studying a pulse-type electric fish, which lends itself to the measurement of sensory sampling. The existence of two distinct states in sensory sampling can be explained by the high metabolic cost of maintaining the EODs (Salazar et al., 2013); thus, animals save significant energy by switching to lower sensory sampling rates at rest. Unlike motor activities, sensory processing in the brain is normally hidden from outside observers, but in *Gymnotus* sp., transitions between two distinct modes of sensory sampling provide a window to the internal sensory dynamics from spontaneously behaving animals for extended periods. In general, active sensing behaviours such as whisking, touching and sniffing are coupled to physical movements such as locomotion (Nelson and MacIver, 2006) or respiration cycles (Wachowiak, 2011), which confound the interpretation of the exact temporal relationship between sensory sampling and movements. Electrosensory sampling activity can be modulated in the absence of physical movements, which offers a unique opportunity to determine the precise temporal relationship between the two.

The nature of volition from a comparative perspective

The nature of volition has been a long-standing inquiry throughout human history, but the discussions remained largely philosophical until the advent of modern tools to monitor brain activity. Discovery

The Journal of Experimental Biology (2014) doi:10.1242/jeb.105502

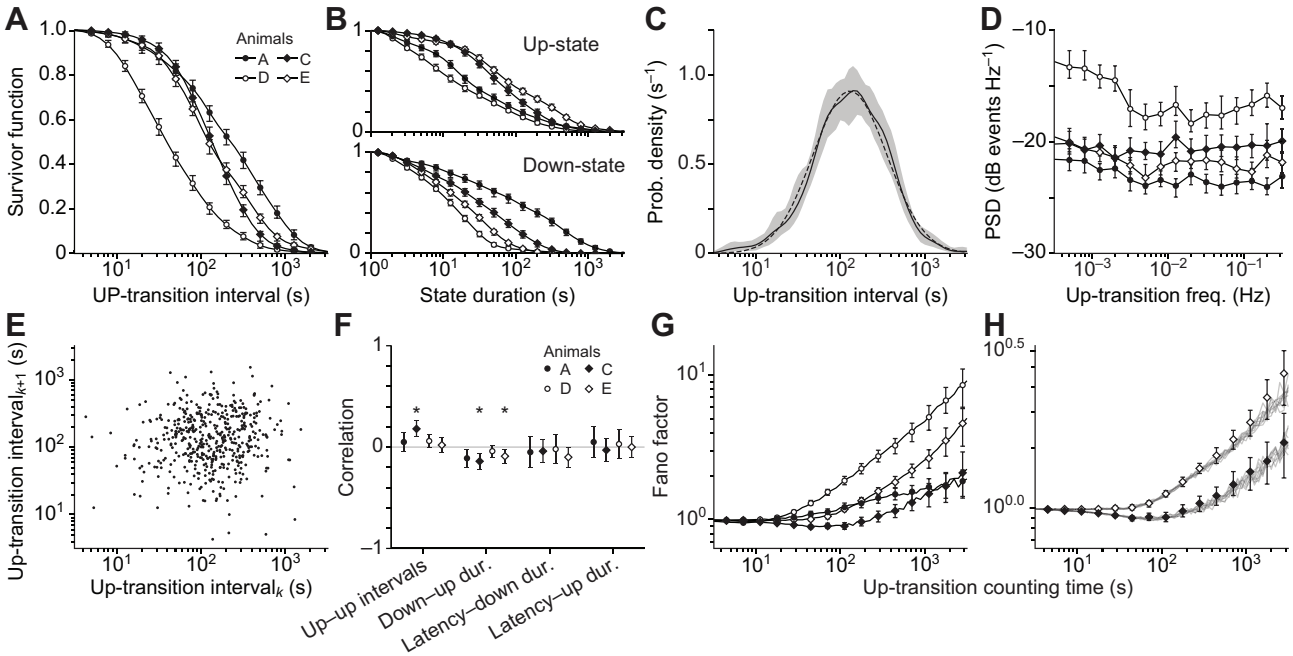

Fig. 8. Spontaneous behavioural transitions follow a random distribution and lack temporal structure. (A,B) Survivor functions (=1–cumulative distribution function) of the log-intervals between two successive up-transitions (A), and log-durations of up- and down-states (B) showed downward linear trends for all four animals. The symbols for each animal are consistent throughout this figure. (C) Distribution of the up-transition intervals from the same animal (solid black line) were well fitted by a log-normal distribution (dashed black line). Shaded areas indicate 99% bootstrap confidence intervals. (D) Power spectral density (PSD) of the up-transition events in the log-frequency domain exhibited approximately equal power at all frequencies, suggesting no characteristic time-scale. (E) No significant temporal correlation exists between two successive log-intervals between spontaneous up-transitions from the same animal. (F) Temporal correlations (Pearson) between successive spontaneous transitions were mostly absent or statistically insignificant; *P<0.01. Up–up intervals, two successive intervals between Up-transitions; Down–up dur., durations of a down-state and a following up-state; Latency–down dur., transition latency and duration of a preceding down-state; Latency–up dur., transition latency and duration of a following up-state. (G) Fano factors for the up-transition counts showed linearly increasing trends on a log–log scale in all four animals. (H) The original Fano factors do not significantly differ from 10 randomly shuffled controls from the same animal (grey lines), indicating lack of temporal structure. Errors bars represent 95% bootstrap confidence interval.

of the readiness potential preceding voluntary action (Kornhuber and Deecke, 1965; Libet et al., 1983) started the quantitative investigation of brain activity during volitional decision making in humans. Prolonged preparatory neural activities characteristic to human voluntary actions are also found in diverse species including monkeys (Romo and Schultz, 1987; Kato et al., 1995; Kaufman et al., 2010) and rodents (Friedman et al., 2006); this suggests that the ability to self-initiate movement is a quantifiable biological trait shared across many vertebrate species including teleost fish. The experience of agency is essential for human volitional actions (Haggard, 2008), and the pre-supplementary motor area is shown to be activated when human subjects pay attention to their intention to act (Lau et al., 2004). However, it is not clear whether non-human animals also share the sense of agency and, if so, how to measure their intention to move. As the awareness of self exists in relation to the external world, the nature of interactions between enhanced sensory sampling and therefore possibly awareness and motor intention (Liu et al., 2010) may lead to a better understanding of volition.

Functional significance of preparatory sensory acquisition and behavioural variability

Before animals decide to move, they must accumulate sufficient information about their sensory surroundings to minimize predation risks, or to optimize foraging decisions. As the preparatory sensory acquisition before movement offers substantial evolutionary advantages, it may be a general feature of the vertebrate brain. Recent studies in humans found a link between preparatory visual sampling and voluntary eye movements, by measuring fixational saccades occurring before the stimulus appearance that signalled voluntary gaze (Watanabe et al., 2013). A sustained period of heightened sensory sampling during movement preparation could improve the detectability of weak or infrequent sensory signals in a noisy background that might be biologically important (Ratnam and Nelson, 2000; Gussin et al., 2007). Given that the increased sensory sampling almost always preceded voluntary movements (Fig. 4E), we propose that heightened sensory acquisition is critical for voluntary decision making.

It has been proposed that variability in spontaneous animal behaviours is an evolutionary necessity, as any form of predictability can be exploited by predators (Jabłoński and Strausfeld, 2000; Catania, 2009). In support of this idea, the spontaneous transitions between down- and up-states exhibited considerable randomness (Fig. 8A–D), and the onset of voluntary movement could not be predicted from its past, or from the duration of the preparatory sensory sampling (Fig. 8E–H). Furthermore, the time course of sensory sampling preceding voluntary movement showed significantly greater variability across trials in comparison to the sensory-evoked condition (Fig. 6D,E). This evidence suggests that although the active sensing behaviour exposes the animal's motor intention to external observers, the intrinsic variability in the preparatory sensory sampling impedes accurate prediction of a movement onset.

Potential neural mechanism for preparatory enhancement of sensory sampling

What neural mechanism could explain preparatory increase in the sensory sampling rate and trial-to-trial variability, and what is the

The Journal of Experimental Biology (2014) doi:10.1242/jeb.105502

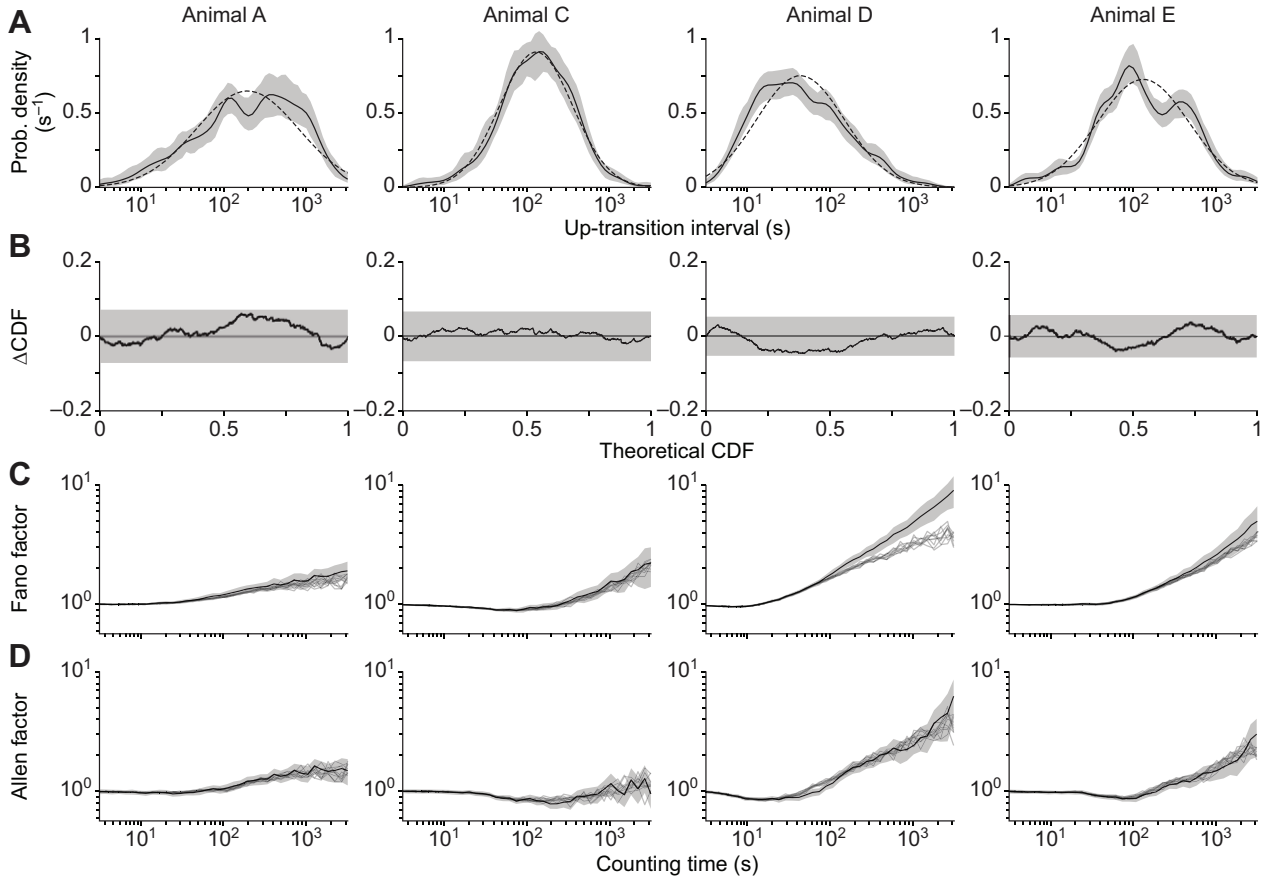

Fig. 9. Distributions of the intervals between spontaneous up-transitions for each animal. (A) Distributions of the up-transition intervals. Shaded areas indicate 99% bootstrap confidence intervals, and dashed black lines indicate log-normal distribution fitting. (B) Kolmogorov–Smirnov (KS) plots of the empirical versus ΔCDF (=empirical CDF–theoretical CDF, where CDF is cumulative distribution function). Shaded areas indicate 99% confidence interval for the paired KS test between the empirical and theoretical CDF (log-normal distribution). (C,D) Log–log plots of the Fano (C) and Allan factors (D) of the up-transition counts. Shaded areas indicate 95% bootstrap confidence intervals, and grey traces indicate 10 randomly shuffled controls.

link between the behavioural transitions and neural activity states (Gervasoni et al., 2004; Mohajerani et al., 2013)? Voluntary movements in primates are associated with preparatory neural activity in the cortex, whereas external sensory stimuli can trigger brainstem reflexes such as the orienting reflex (Sokolov, 1990) and novelty responses (Caputi et al., 2003) without necessary cortical activation. Acoustic stimulation likely increases the EODR via brainstem interneurons (Korn and Faber, 2005; Comas and Borde, 2010), whereas the neural substrates of self-initiated movements in *Gymnotus* sp. are not currently known. We suspect that they will

Table 3. Data summary for the spontaneous up-transitions

	A	B	C	D	E
No. up-transitions	517	322	595	965	819
Log-normal distribution fitting parameters (mean, s.d.) for up-transition log-intervals[a]	5.27±0.12, 1.42±0.09	4.35±0.10, 0.96±0.07	4.87±0.08, 1.01±0.06	3.78±0.08, 1.22±0.05	4.88±0.09,
Correlation between successive up-transition intervals[a]	0.05±0.09, P=0.2494	0.09±0.11, P=0.0974	0.18±0.08, P=0.0000	0.06±0.06, P=0.0811	0.02±0.07, P=0.6472
Correlation between successive down- and up-state durations[a]	−0.11±0.09, P=0.0127	−0.13±0.11, P=0.0210	−0.14±0.08, P=0.0009	−0.04±0.06, P=0.1909	−0.09±0.07, P=0.0079
Correlation between transition latency and down-state duration	−0.05±0.15, P=0.4717	−0.03±0.14, P=0.6544	−0.04±0.11, P=0.5128	−0.02±0.14, P=0.8047	−0.10±0.10, P=0.0493
Correlation between transition latency and up-state duration	0.05±0.15, P=0.4972	0.14±0.14, P=0.0475	−0.03±0.11, P=0.5780	0.03±0.14, P=0.6976	−0.00±0.10, P=0.9294
Fano factor slope[b]	0.13±0.01	N/A[e]	0.21±0.04	0.44±0.01	0.37±0.02
Allan factor slope[c]	0.13±0.02	N/A[e]	0.17±0.04	0.37±0.03	0.26±0.02
Hurst exponent[d]	0.54±0.01	N/A[e]	0.52±0.01	0.63±0.02	0.56±0.02

Data are given for animals A–E. Data for up- and down-state EODR and EODA are means ± s.d.
[a]95% confidence interval is given. [b]Lines were fitted to log–log plots between t=$10^{0.2}$ and $10^{3.5}$ s for all animals. [c]Lines were fitted to log–log plots between t=$10^{0.2}$ and $10^{3.5}$ s for animals A, B and E; t=$10^{2.25}$ and $10^{3.5}$ s for animal C; and t=$10^{1.75}$ and $10^{3.5}$ s for animal D. [d]Lines were fitted to log–log plots (s.d. versus time) between t=$10^{0.5}$ and $10^{3.5}$ s for all animals. [e]Data from animal B were insufficient to compute the Fano and Allan factors, and the Hurst exponent.

include telencephalic regions (Braithwaite, 2005) that are likely homologous with the mammalian pallium and basal ganglia (Wong, 1997; Harvey-Girard et al., 2012; Harvey-Girard et al., 2013). A recent paper (Pereira et al., 2014) has demonstrated that when the telencephalon of *Gymnotus omarum* is ablated the fish remains quiescent and does not initiate movement for the duration of lengthy experiments. This supports our hypothesis that the telencephalon is required to initiate movement. Further support for this idea is that blocking inhibition in the dorsolateral pallium of *Gymotus carapo* (Santana et al., 2001) induces striking changes in the patterning of its EOD. The dorsolateral pallium is known to receive highly processed electrosensory input and might be able to modulate both the EODR and locomotion via its output to midbrain regions including the tectum (Giassi et al., 2012). However, while the pallium is a reasonable candidate, the ultimate neural basis of enhanced sensory acquisition preceding voluntary movement remains unknown, as well as the nature of interactions between the microcircuits for sensory evaluation and motor planning. It has been shown that forebrain stimulations enhanced visual spatial attention in the barn owl (Winkowski and Knudsen, 2006), and hypothalamic stimulation triggered head-scanning behaviours followed by locomotion in mice (Sinnamon et al., 1999), suggesting additional candidate regions involved in the initiation of enhanced sensory sampling before movement.

Conclusions

Our study shows that *Gymnotus* sp. can, in the absence of any extraneous input, switch between inactive (down) and active (up) states. The self-initiated onsets of up-states occur randomly and, as they are associated with an increased sensory sampling rate, we hypothesize that they are exploratory behaviours during which the animal is in a heightened sensory state. Haggard (Haggard, 2008) has suggested that voluntary actions in humans are a form of 'decision making' with two special characteristics: they are exploratory behaviours that are not directly triggered by sensory input but, rather, occur in a random fashion. Our study reveals that the self-initiated movements of *Gymnotus* sp. have these characteristics of voluntary actions. The connection between volition and decision making is reinforced by the fact that neural activity, as reflected in the EODR, precedes self-initiated movements by a time scale comparable to that of the preparatory cortical activity in humans (Kornhuber and Deecke, 1965; Libet et al., 1983). Finally, consistent with the studies in mammals reporting that neural variability decreases after voluntary action (Steinmetz and Moore, 2010; Churchland et al., 2011) or stimulus onset (Steinmetz and Moore, 2010; Churchland et al., 2010), the sensory sampling variability in our animals followed the same decline under the two conditions. We conclude that not only may *Gymnotus* sp. exhibit volition but also neural processing preceding the decision to move might also bear some similarity to that in humans according to their similar temporal dynamics. Given the substantial homologies between the telencephali of teleost fish and mammals (Braithwaite, 2005; Harvey-Girard et al., 2012; Harvey-Girard et al., 2013), locating the brain regions that trigger the up-states in *Gymnotus* sp. may give clues as to the initiation sites of human voluntary actions. In turn, this may expose the circuitry controlling sensory acquisition rates and their possible relation to decision-making mechanisms (Gold and Shadlen, 2007; Heekeren et al., 2008).

MATERIALS AND METHODS

Gymnotus sp. were housed in a circular tank surrounded by a sensory-isolation chamber to block external sources of light, sound and vibration. The animals were under a 12 h light cycle, and recordings were made in darkness during the active part of the fish circadian rhythm. Water filtration, aeration and feeding were performed between recording sessions. EOD pulse times were precisely and reliably recorded as previously described (Jun et al., 2012). Movement activity level was determined from the slopes of the EOD peak amplitudes (Jun et al., 2013). During sound-evoked trials, acoustic stimuli were delivered at random intervals to prevent habituation.

Experimental animals

All procedures including housing and recording protocols were approved by the University of Ottawa Animal Care Committee. We obtained South American pulse-type weakly electric fish (genus *Gymnotus*) of unknown species and sex from a local supplier (Big Al aquarium services, Ottawa, ON, Canada). After arrival, animals were initially housed in a community tank, and fed live blackworms prior to experimental observation. Animals were brought to the experimental tank one at a time, and acclimatized for at least 2 days before the first recording. Animals were individually housed and maintained on a 12 h light cycle with *ad libitum* access to food (mealworms) except for the recording duration. Experiments were performed in the dark cycle.

Experimental setup

The experimental tank and isolation chamber were as previously described (Fig. 1A) (Jun et al., 2012; Jun et al., 2014). Underwater sound was recorded during experiments by a hydrophone (TC4013, Reson Inc., Goleta, CA, USA) and amplified (50 dB gain; VP1000, Reson Inc.) to check for animal movements triggered by external vibrations. Detailed descriptions of the experimental chamber, the aquarium tank designs and water conditions are provided elsewhere (Jun et al., 2014).

EOD recording and movement activity

The EOD signals were recorded from multiple electrodes, which reliably and accurately captured the animal's EOD pulses at all tank locations [see Jun et al. (Jun et al., 2012) for our EOD pulse detection technique]. The EODR was determined by smoothing the instantaneous EOD pulse rate (averaging filter, τ=0.0625 s), and was linearly interpolated at a constant sampling rate (100 Hz) to facilitate data synchronization and subsequent analysis. The EOD amplitudes conveyed movement information, as the animal's movements caused fluctuations of the EOD amplitudes at the recording electrodes (Jun et al., 2012). We quantified the activity level of an animal by integrating the EOD amplitude fluctuations from all recording channels. The activity level computed from the EOD recording accurately quantified the animal's movements without requiring a concurrent video recording, which demands significantly greater storage space due to high-speed and high-resolution imaging for sensitive motion detection [see Jun et al. (Jun et al., 2014) for the method of computing the activity level].

State segregation method

The fish's movement activities and sensory sampling rates both followed well-defined bimodal distributions that were highly temporally correlated (Fig. 1G). Because of their binary nature, we divided the behavioural time series into two states in order to characterize the two states and the state transitions, according to the following procedures. First, principal component analysis was performed to compute the first principal component (PC1) of EODR and activity level. Second, the state segregation was performed based on the PC1 score, as its distribution exhibited greater separation between the two modes than either of the original measures (Fig. 1H). To evaluate the goodness of separation, a separation index (SI) was computed for each distribution as follows:

$$\mathrm{SI} = \frac{|\,\mathrm{Mode}_1 - \mathrm{Mode}_2\,|}{\sqrt{\mathrm{FWHM}_1 \times \mathrm{FWHM}_2}}, \quad (1)$$

where the subscripts 1 and 2 refer to the first and second peaks; FWHM, full width half-maximum. Out of the three distributions (EODR, activity level and PC1), the SI was the highest for the PC1 distribution for 20 out of 23 recording sessions. For each recording day, a threshold level for the PC1

score was determined at the local minimum of its bimodal distribution between the two peaks. Recordings with predominantly up- or down-states (i.e. where up- or down-states occupied more than 90% of the data) generally occurred during initial acclimation periods, and were excluded from analysis (30% of all recording sessions) because of greater overlap in the bimodal distribution and inaccurate state segregation. The states were initially divided by applying a threshold; subsequently, transient up-states lasting less than 1.5 s were merged with their neighbouring down-states, and vice versa for the transient down-states (Fig. 2A). The 1.5 s cut-off was determined from the first local minimum (Ji and Wilson, 2007) of the up-state duration histogram (Fig. 2B, left). After the state segregation, the EODR and activity level were normalized to facilitate pooling data from multiple days and animals, which originally exhibited different baselines (Fig. 1I). The median values during down- and up-states were mapped to zero and one, respectively, by linearly rescaling both EODR and activity level (Fig. 2C). In essence, the normalization procedure expressed the movement activity and sensory sampling rate measures on a standardized scale corresponding to the two states, regardless of their characteristic distributions. We refer to the EODR and activity level in the normalized unit throughout this paper unless otherwise stated.

Movement-onset triggered analysis

The up-transition times determined from the PC1 score did not accurately correspond to the actual movement-onset times, as the PC1 score is also based on EODR, which does not directly quantify movements. Therefore, we refined the movement-onset times by using the normalized activity level that directly quantifies movement. The temporal precision of the EOD-based movement-onset times was improved to the level of a visual detection method (Fig. 5A–F) by applying the following procedures (Jun et al., 2014). First, we selected a subset of up-transitions exhibiting clearly discernible movement onset and clear down- and up-states based on the following criteria. The down- and up-state durations had to last longer than 5 s each; the averaged normalized activity level had to be under 0.1 between 0 and 1 s before movement onset, and over 0.6 between 0 and 1 s after movement onset for the down- and up-states, respectively. The first threshold crossing of the activity level within 5 s of the PC1 up-transition onset (or sound onset times during evoked trials) was taken as the movement-onset time, and the threshold (0.2) was chosen at the mean local minimum of the bimodal distribution of the normalized activity level. Similarly, the EODR rise-onset times were determined at the first threshold crossing (0.4) of the normalized EODR within 5 s of the up-transition. The transition latency was computed by taking the difference between the EODR rise onset and the movement-onset times.

We did not analyse movement offsets, as it was difficult to determine the exact moment because of the inertia of the fish's body. The movement-onset times determined by the EOD recordings were verified by concurrent visual recordings from animal B, and a mean corrective time offset (25 ms) was subtracted from the EOD-based movement-onset times to minimize the average timing error. In order to check for the effect of external acoustic and vibratory noise on animal movements, the hydrophone recording traces were (1) notch-filtered (f_c=60 Hz, Q=10) and rms filtered (τ=0.1 s) to remove the mains interference, (2) aligned at the movement-onset times (Fig. 4C) and (3) averaged across trials after subtracting the mean (±5 s from the movement onset; Fig. 4D). Averaging did not lead to the cancellation of sound waves having different phases, as the rms filter extracted the waveform envelope.

Video calibration

In selected trials, we simultaneously recorded infrared videos from animal B to validate and calibrate movement-onset times determined from the EOD recordings (activity level threshold crossing). During video recordings, the experimental chamber was illuminated by eight infrared LED lights (λ=880 nm) invisible to teleost fish (Fernald, 1988; Douglas and Hawryshyn, 1990). A modified webcam (infrared blocking filter was removed; C910, Logitech, Fremont, CA, USA) captured video (15 frames s^{-1}, 640×480) from directly above the tank using Spike2 software (CED, Cambridge, UK). Video recordings were synchronized with the EOD recordings by periodically blinking an infrared LED (10 ms duration, 10 s interval), and the light pulse timing was simultaneously captured by the digitizer. The first and last light pulses captured by the camera were used to convert the image frame numbers to the digitizer time unit, and vice versa. After determining movement-onset times from the EOD recordings, each movement-onset time was independently confirmed by concurrent video recording according to the following procedures. (1) Image frames within 5 s of the EOD-based movement-onset times were loaded to memory. (2) A reference region-of-interest (ROI) was defined by drawing a polygon around an animal image on the first frame. (3) Spatially averaged Pearson correlation coefficients were calculated for the pixel values in the reference ROI and all the rest of the image frames. (4) An image frame number was manually marked when the averaged correlation coefficient began to decrease significantly, indicating a movement onset (Fig. 5A). The differences between the EOD-based and visually determined movement-onset times were calculated to quantify the temporal precision of the movement-onset detection (Fig. 5B–E), and to calibrate the EOD-based movement-onset times. We quantified the relationship between the activity level and log-speed (Fig. 5F). The speed of animal centroid was determined by custom-made MATLAB (The MathWorks, Natick, MA, USA) image tracking software (Jun et al., 2014), and the minimum speed was set to 1 cm s^{-1} before applying the log transformation.

Acoustic stimuli

In order to compare increases in of the EOD rates associated with spontaneous movements with those associated with sensory-evoked responses, we delivered loud acoustic stimuli (143 dB SPL re. 1 µPa rms) at random intervals (5±1 min) to trigger startle movements. Brief pure-tone acoustic stimuli (0.5 or 1 s duration, 150 Hz) were delivered by two 200 W subwoofers (Z623, Logitech), which rested on foam bases (5.1 cm thick) above the experimental tank and faced upward to minimize acoustic interference between the two speakers. The sound intensity was calibrated by a hydrophone (TC4013, Reson) positioned 3 cm below the water surface at various tank locations, and the spatial variation of the sound intensity was within 10% from the mean. Delivery of the acoustic stimuli was controlled by the digitizer software (Spike2, CED), and the inter-stimuli intervals were drawn from a uniform random distribution (5±1 min) to prevent habituation (Post and von der Emde, 1999). The acoustic stimuli always triggered stereotyped novelty responses within a single EOD pulse cycle from the stimulus onset; however, the acoustic stimuli did not always trigger sufficiently large movements (<30% of all trials). To generate movement-onset-triggered plots (Fig. 4A,B), we pooled trials exhibiting significant movements (activity level >0.325) within 1 s of the stimulus onset; but all trials were pooled for calculating the stimulus-triggered averages and s.d. (Fig. 6A–D, Fig. 7A–C) and the CV of EOD intervals (Fig. 6G). The acoustic stimuli were delivered in darkness, and we only analysed trials when animals exhibited clear resting baselines (activity level <0.1 and EODR <0.4) between 0 and 1 s before the stimulus onset.

Statistical analyses

The probability distribution of the EODR and EODA (Fig. 2A,C) was estimated by applying a kernel smoothing method (*ksdensity* function in MATLAB), and all other probability distributions and cumulative distributions were estimated this way (e.g. Fig. 8A–C, Fig. 9A). The error bars in all probability and cumulative distribution plots indicate 95% confidence intervals, and were estimated by applying a bootstrap sampling method (*bootci* function in MATLAB). The error bars in all trial-averaged plots indicate means ± s.e.m. (e.g. Fig. 4A–D, Fig. 6E). Because of the lack of hydrophone recordings, Animal A was excluded from generating the movement-triggered background noise plot (Fig. 4D). Animal B was excluded from generating the spontaneous transition statistics (Fig. 8A,B,D–G, Fig. 9A–D) because of insufficient total recording hours (under 11 h). We pooled 1319 trials from five animals under the spontaneous condition, and 261 trials were pooled from five animals under the evoked condition to compute the trial-to-trial variability over time (Fig. 6G). During spontaneous and evoked transitions (within 5 s of movement or stimulus onset), trials exhibiting transient EOD interruptions (Schuster, 2002) were automatically excluded. Trials showing the normalized EODR below the

threshold (−1) were removed, which constituted less than 1% of the total number of trials.

Acknowledgements
We thank Drs Erik S. Fortune, Jorge Mejias and Richard Naud for their helpful suggestions.

Competing interests
The authors declare no competing financial interests.

Author contributions
L.M. and J.J.J. conceived, planned and designed experiments. J.J.J. performed experiments, data analysis, and drafted the manuscript. L.M. and A.L. contributed to the data analysis and writing.

Funding
This project was funded by the Natural Sciences and Engineering Research Council of Canada (grant no. 121891-2009 to A.L.; NSERC PGS scholarship to J.J.J.), and by the Canadian Institutes of Health Research (grant no. 49510 to L.M. and A.L.).

Supplementary material
Supplementary material available online at
http://jeb.biologists.org/lookup/suppl/doi:10.1242/jeb.105502/-/DC1

References

Arnegard, M. E. and Carlson, B. A. (2005). Electric organ discharge patterns during group hunting by a mormyrid fish. *Proc. Biol. Sci.* **272**, 1305-1314.
Barrio, L. C., Caputi, A., Crispino, L. and Buno, W. (1991). Electric organ discharge frequency-modulation evoked by water vibration in *Gymnotus carapo*. *Comp. Biochem. Physiol.* **100A**, 555-562.
Braithwaite, V. A. (2005). Cognitive ability in fish. *Fish Physiol.* **24**, 1-37.
Brown, E. N., Barbieri, R., Ventura, V., Kass, R. E. and Frank, L. M. (2002). The time-rescaling theorem and its application to neural spike train data analysis. *Neural Comput.* **14**, 325-346.
Caputi, A., Silva, A. A. and Macadar, O. (1993). Electric organ activation in Gymnotus carapo: spinal origin and peripheral mechanisms. *J. Comp. Physiol. A* **173**, 227-232.
Caputi, A. A., Aguilera, P. A. and Castelló, M. E. (2003). Probability and amplitude of novelty responses as a function of the change in contrast of the reafferent image in G carapo. *J. Exp. Biol.* **206**, 999-1010.
Catania, K. C. (2009). Tentacled snakes turn C-starts to their advantage and predict future prey behavior. *Proc. Natl. Acad. Sci. USA* **106**, 11183-11187.
Churchland, M. M., Yu, B. M., Cunningham, J. P., Sugrue, L. P., Cohen, M. R., Corrado, G. S., Newsome, W. T., Clark, A. M., Hosseini, P., Scott, B. B. et al. (2010). Stimulus onset quenches neural variability: a widespread cortical phenomenon. *Nat. Neurosci.* **13**, 369-378.
Churchland, A. K., Kiani, R., Chaudhuri, R., Wang, X. J., Pouget, A. and Shadlen, M. N. (2011). Variance as a signature of neural computations during decision making. *Neuron* **69**, 818-831.
Comas, V. and Borde, M. (2010). Neural substrate of an increase in sensory sampling triggered by a motor command in a gymnotid fish. *J. Neurophysiol.* **104**, 2147-2157.
Desmurget, M. and Sirigu, A. (2012). Conscious motor intention emerges in the inferior parietal lobule. *Curr. Opin. Neurobiol.* **22**, 1004-1011.
Douglas, R. H. and Hawryshyn, C. W. (1990). Behavioral studies of fish vision: an analysis of visual capabilities. In *The Visual System of Fish* (ed. R. H. Douglas and M. B. A. Djamgoz), pp. 373-418. London: Chapman & Hall.
Dye, J. (1988). An in vitro physiological preparation of a vertebrate communicatory behavior: chirping in the weakly electric fish, Apteronotus. *J. Comp. Physiol. A* **163**, 445-458.
Fernald, R. D. (1988**).** Aquatic adaptations in fish eyes. In *Sensory Biology of Aquatic Animals* (ed. J. Atema, R. R. Fay, A. N. Popper and W. Tarolga), pp. 435-466. New York, NY: Springer-Verlag.
Fried, I., Mukamel, R. and Kreiman, G. (2011). Internally generated preactivation of single neurons in human medial frontal cortex predicts volition. *Neuron* **69**, 548-562.
Friedman, W. A., Jones, L. M., Cramer, N. P., Kwegyir-Afful, E. E., Zeigler, H. P. and Keller, A. (2006). Anticipatory activity of motor cortex in relation to rhythmic whisking. *J. Neurophysiol.* **95**, 1274-1277.
Gebber, G. L., Orer, H. S. and Barman, S. M. (2006). Fractal noises and motions in time series of presympathetic and sympathetic neural activities. *J. Neurophysiol.* **95**, 1176-1184.
Gervasoni, D., Lin, S. C., Ribeiro, S., Soares, E. S., Pantoja, J. and Nicolelis, M. A. (2004). Global forebrain dynamics predict rat behavioral states and their transitions. *J. Neurosci.* **24**, 11137-11147.
Giassi, A. C., Duarte, T. T., Ellis, W. and Maler, L. (2012). Organization of the gymnotiform fish pallium in relation to learning and memory: II. Extrinsic connections. *J. Comp. Neurol.* **520**, 3338-3368.
Gold, J. I. and Shadlen, M. N. (2007). The neural basis of decision making. *Annu. Rev. Neurosci.* **30**, 535-574.
Gussin, D., Benda, J. and Maler, L. (2007). Limits of linear rate coding of dynamic stimuli by electroreceptor afferents. *J. Neurophysiol.* **97**, 2917-2929.
Haggard, P. (2008). Human volition: towards a neuroscience of will. *Nat. Rev. Neurosci.* **9**, 934-946.
Hardstone, R., Poil, S. S., Schiavone, G., Jansen, R., Nikulin, V. V., Mansvelder, H. D. and Linkenkaer-Hansen, K. (2012). Detrended fluctuation analysis: a scale-free view on neuronal oscillations. *Front. Physiol.* **3**, 450.
Harvey-Girard, E., Giassi, A. C. C., Ellis, W. and Maler, L. (2012). Organization of the gymnotiform fish pallium in relation to learning and memory: IV. Expression of conserved transcription factors and implications for the evolution of dorsal telencephalon. *J. Comp. Neurol.* **520**, 3395-3413.
Harvey-Girard, E., Giassi, A. C. C., Ellis, W. and Maler, L. (2013). Expression of the cannabinoid CB1 receptor in the gymnotiform fish brain and its implications for the organization of the teleost pallium. *J. Comp. Neurol.* **521**, 949-975.
Heekeren, H. R., Marrett, S. and Ungerleider, L. G. (2008). The neural systems that mediate human perceptual decision making. *Nat. Rev. Neurosci.* **9**, 467-479.
Heiligenberg, W. (1980). The evaluation of electroreceptive feedback in a Gymnotid fish with a pulse-type electric organ discharge. *J. Comp. Physiol.* **138**, 173-185.
Heiligenberg, W., Finger, T., Matsubara, J. and Carr, C. (1981). Input to the medullary pacemaker nucleus in the weakly electric fish, *Eigenmannia* (Sternopygidae, Gymnotiformes). *Brain Res.* **211**, 418-423.
Hopkins, C. D. (1983). Functions and mechanisms in electroreception. In *Fish Neurobiology* (ed. R. G. Northcutt and R. E. Davis), pp. 215-259. Ann Arbor, MI: University of Michigan Press.
Jabłoński, P. G. and Strausfeld, N. J. (2000). Exploitation of an ancient escape circuit by an avian predator: prey sensitivity to model predator display in the field. *Brain Behav. Evol.* **56**, 94-106.
Ji, D. and Wilson, M. A. (2007). Coordinated memory replay in the visual cortex and hippocampus during sleep. *Nat. Neurosci.* **10**, 100-107.
Jun, J. J., Longtin, A. and Maler, L. (2012). Precision measurement of electric organ discharge timing from freely moving weakly electric fish. *J. Neurophysiol.* **107**, 1996-2007.
Jun, J. J., Longtin, A. and Maler, L. (2013). Real-time localization of moving dipole sources for tracking multiple free-swimming weakly electric fish. *PLoS ONE* **8**, e66596.
Jun, J. J., Longtin, A. and Maler, L. (2014). Long-term behavioral tracking of freely swimming weakly electric fish. *J. Vis. Exp.* **83**, e50962.
Kato, M., Miyashita, N., Hikosaka, O., Matsumura, M., Usui, S. and Kori, A. (1995). Eye movements in monkeys with local dopamine depletion in the caudate nucleus. I. Deficits in spontaneous saccades. *J. Neurosci.* **15**, 912-927.
Kaufman, M. T., Churchland, M. M., Santhanam, G., Yu, B. M., Afshar, A., Ryu, S. I. and Shenoy, K. V. (2010). Roles of monkey premotor neuron classes in movement preparation and execution. *J. Neurophysiol.* **104**, 799-810.
Kawasaki, M., Maler, L., Rose, G. J. and Heiligenberg, W. (1988). Anatomical and functional organization of the prepacemaker nucleus in gymnotiform electric fish: the accommodation of two behaviors in one nucleus. *J. Comp. Neurol.* **276**, 113-131.
Kleinfeld, D., Ahissar, E. and Diamond, M. E. (2006). Active sensation: insights from the rodent vibrissa sensorimotor system. *Curr. Opin. Neurobiol.* **16**, 435-444.
Korn, H. and Faber, D. S. (2005). The Mauthner cell half a century later: a neurobiological model for decision-making? *Neuron* **47**, 13-28.
Kornhuber, H. H. and Deecke, L. (1965). Hirnpotentialänderungen bei willkürbewegungen und passiven bewegungen des menschen: bereitschaftspotential und reafferente potentiale. *Pflugers Arch.* **284**, 1-17.
Lau, H. C., Rogers, R. D., Haggard, P. and Passingham, R. E. (2004). Attention to intention. *Science* **303**, 1208-1210. </jrn>
Libet, B., Gleason, C. A., Wright, E. W. and Pearl, D. K. (1983). Time of conscious intention to act in relation to onset of cerebral activity (readiness-potential). The unconscious initiation of a freely voluntary act. *Brain* **106**, 623-642.
Lissmann, H. W. and Schwassmann, H. O. (1965). Activity rhythm of an electric fish, *Gymnorhamphichthys hipostomus*. *Z. Vergl. Physiol.* **51**, 153-171.
Litwin-Kumar, A. and Doiron, B. (2012). Slow dynamics and high variability in balanced cortical networks with clustered connections. *Nat. Neurosci.* **15**, 1498-1505.
Liu, Y., Yttri, E. A. and Snyder, L. H. (2010). Intention and attention: different functional roles for LIPd and LIPv. *Nat. Neurosci.* **13**, 495-500.
Metzner, W. (1993). The jamming avoidance response in Eigenmannia is controlled by two separate motor pathways. *J. Neurosci.* **13**, 1862-1878.
Metzner, W. (1999). Neural circuitry for communication and jamming avoidance in gymnotiform electric fish. *J. Exp. Biol.* **202**, 1365-1375.
Mohajerani, M. H., Chan, A. W., Mohsenvand, M., LeDue, J., Liu, R., McVea, D. A., Boyd, J. D., Wang, Y. T., Reimers, M. and Murphy, T. H. (2013). Spontaneous cortical activity alternates between motifs defined by regional axonal projections. *Nat. Neurosci.* **16**, 1426-1435.
Moller, P. (1995). *Electric Fishes. History and Behavior*. London: Chapman & Hall.
Nawrot, M. P., Boucsein, C., Rodriguez Molina, V., Riehle, A., Aertsen, A. and Rotter, S. (2008). Measurement of variability dynamics in cortical spike trains. *J. Neurosci. Methods* **169**, 374-390.
Nelson, M. E. and MacIver, M. A. (2006). Sensory acquisition in active sensing systems. *J. Comp. Physiol. A* **192**, 573-586.
Otero-Millan, J., Troncoso, X. G., Macknik, S. L., Serrano-Pedraza, I. and Martinez-Conde, S. (2008). Saccades and microsaccades during visual fixation, exploration, and search: foundations for a common saccadic generator. *J. Vis.* **8**, 21.
Pereira, A. C., Rodríguez-Cattáneo, A. and Caputi, A. A. (2014). The slow pathway in the electrosensory lobe of Gymnotus omarorum: Field potentials and unitary activity. *J. Physiol.* (in press).

Pluta, S. R. and Kawasaki, M. (2008). Multisensory enhancement of electromotor responses to a single moving object. *J. Exp. Biol.* **211**, 2919-2930.
Post, N. and von der Emde, G. (1999). The 'novelty response' in an electric fish: response properties and habituation. *Physiol. Behav.* **68**, 115-128.
Poulet, J. F. and Petersen, C. C. (2008). Internal brain state regulates membrane potential synchrony in barrel cortex of behaving mice. *Nature* **454**, 881-885.
Proekt, A., Banavar, J. R., Maritan, A. and Pfaff, D. W. (2012). Scale invariance in the dynamics of spontaneous behavior. *Proc. Natl. Acad. Sci. USA* **109**, 10564-10569.
Ratnam, R. and Nelson, M. E. (2000). Nonrenewal statistics of electrosensory afferent spike trains: implications for the detection of weak sensory signals. *J. Neurosci.* **20**, 6672-6683.
Romo, R. and Schultz, W. (1987). Neuronal activity preceding self-initiated or externally timed arm movements in area 6 of monkey cortex. *Exp. Brain Res.* **67**, 656-662.
Salazar, V. L., Krahe, R. and Lewis, J. E. (2013). The energetics of electric organ discharge generation in gymnotiform weakly electric fish. *J. Exp. Biol.* **216**, 2459-2468.
Santana, U. J., Roque-da-Silva, A. C., Duarte, T. T. and Corrêa, S. A. L. (2001). Interference with the GABAergic system in the dorsolateral telencephalon and modulation of the electric organ discharge frequency in the weakly electric fish Gymnotus carapo. *J. Comp. Physiol. A* **187**, 925-933.
Schroeder, C. E., Wilson, D. A., Radman, T., Scharfman, H. and Lakatos, P. (2010). Dynamics of active sensing and perceptual selection. *Curr. Opin. Neurobiol.* **20**, 172-176.
Schuster, S. (2002). Behavioral evidence for post-pause reduced responsiveness in the electrosensory system of *Gymnotus carapo*. *J. Exp. Biol.* **205**, 2525-2533.
Sinnamon, H. M., Karvosky, M. E. and Ilch, C. P. (1999). Locomotion and head scanning initiated by hypothalamic stimulation are inversely related. *Behav. Brain Res.* **99**, 219-229.
Sokolov, E. N. (1990). The orienting response, and future directions of its development. *Pavlov. J. Biol. Sci.* **25**, 142-150.
Soon, C. S., Brass, M., Heinze, H. J. and Haynes, J. D. (2008). Unconscious determinants of free decisions in the human brain. *Nat. Neurosci.* **11**, 543-545.
Steinmetz, N. A. and Moore, T. (2010). Changes in the response rate and response variability of area V4 neurons during the preparation of saccadic eye movements. *J. Neurophysiol.* **103**, 1171-1178.
Ulanovsky, N. and Moss, C. F. (2008). What the bat's voice tells the bat's brain. *Proc. Natl. Acad. Sci. USA* **105**, 8491-8498.
Wachowiak, M. (2011). All in a sniff: olfaction as a model for active sensing. *Neuron* **71**, 962-973.
Watanabe, M., Matsuo, Y., Zha, L., Munoz, D. P. and Kobayashi, Y. (2013). Fixational saccades reflect volitional action preparation. *J. Neurophysiol.* **110**, 522-535.
Winkowski, D. E. and Knudsen, E. I. (2006). Top-down gain control of the auditory space map by gaze control circuitry in the barn owl. *Nature* **439**, 336-339.
Wong, C. J. H. (1997). Afferent and efferent connections of the diencephalic prepacemaker nucleus in the weakly electric fish, *Eigenmannia virescens*: interactions between the electromotor system and the neuroendocrine axis. *J. Comp. Neurol.* **383**, 18-41.
Zupanc, G. K. H. and Maler, L. (1997). Neuronal control of behavioral plasticity: the prepacemaker nucleus of weakly electric gymnotiform fish. *J. Comp. Physiol. A* **180**, 99-111.